ReGeo ISSN: 2177-3246

PEELING OF THE CERAMIC COATING BY CYCLIC STRESSES

DESPLACAMENTO DO REVESTIMENTO CERÂMICO POR TENSÕES CÍCLICAS

DESPRENDIMIENTO DEL RECUBRIMIENTO CERÁMICO POR TENSIONES CÍCLICAS

10.56238/revgeov17n3-122

João Carlos Barleta Uchôa[1], Marcus Vinícius Araújo da Silva Mendes[2], Carlos Mariano Melo Júnior[3], Luciano Mendes Bezerra[4]

ABSTRACT

The deformations that may occur in the ceramic tilling system caused by weathering and the difference of thermal and hygrometric materials behavior cause tensions between the layers of the ceramic tilling system. Deformations added to the restrictions of the connections of the interfaces between layers generate stresses able to take off the ceramic tilling. Therefore, it was decided to use an experimental approach and numerical analysis to study the fatigue behavior of industrialized adhesive mortar type ACII and ACIII that compose the ceramic tilling system, subjecting to tensile and compressive of cyclic loading. In the experimental approach were carried tensile fatigue tests and axial compression for ACII and ACIII mortars, where the stress levels for achievement of fatigue tests were defined from the results obtained in the tensile strength of characterization tests on bending and the axial compression of these mortars. The results of the fatigue tests were able to allow S-N curve or Wöhler curve were plotted to obtain the rupture limit of fatigue strength to ACII ACIII mortars.

Keywords: Detachment Ceramic Tilling. Fatigue. Mortar.

RESUMO

As deformações que podem ocorrer no sistema de revestimento cerâmico, causadas pelo intemperismo e pelas diferenças no comportamento térmico e higrométrico dos materiais, geram tensões entre as camadas do sistema de revestimento cerâmico. As deformações, somadas às restrições nas ligações das interfaces entre as camadas, geram esforços capazes de provocar o descolamento do revestimento cerâmico. Assim, decidiu-se utilizar uma abordagem experimental e análise numérica para estudar o comportamento à fadiga das argamassas colantes industrializadas do tipo ACII e ACIII que compõem o sistema de

[1] Dr. in Civil Construction Structures. Universidade de Brasília (UnB). Instituto Federal de Educação, Ciência e Tecnologia de Brasília (IFB). E-mail: 1189735@ifb.edu.br

[2] Dr. in Civil Construction Structures. Universidade de Brasília (UnB). Instituto Federal de Educação, Ciência e Tecnologia de Goiás (IFG). E-mail: marcus.mendes@ifg.edu.br

[3] Dr. in Civil Construction Structures . Universidade de Brasília (UnB). Instituto Federal de Educação, Ciência e Tecnologia de Sergipe (IFS). E-mail: carlos.mariano@academico.ifs.edu.br

[4] Dr. in Computational Mechanics. Carnegie Mellon University (USA). Universidade de Brasília (UnB). E-mail: luciano.bezerra@unb.br

revestimento cerâmico, submetendo-as a carregamentos cíclicos de tração e compressão. Na abordagem experimental foram realizados ensaios de fadiga à tração e compressão axial para as argamassas ACII e ACIII, nos quais os níveis de tensão para a realização dos ensaios de fadiga foram definidos a partir dos resultados obtidos nos ensaios de caracterização de resistência à tração na flexão e de compressão axial dessas argamassas. Os resultados dos ensaios de fadiga permitiram a construção da curva S-N ou curva de Wöhler, possibilitando a obtenção do limite de ruptura por fadiga das argamassas ACII e ACIII.

Palavras-chave: Descolamento do Revestimento Cerâmico. Fadiga. Argamassa.

RESUMEN

Las deformaciones que pueden ocurrir en el sistema de revestimiento cerámico, causadas por el intemperismo y por las diferencias en el comportamiento térmico e higrométrico de los materiales, generan tensiones entre las capas del sistema de revestimiento cerámico. Las deformaciones, sumadas a las restricciones en las uniones de las interfaces entre las capas, generan esfuerzos capaces de provocar el desprendimiento del revestimiento cerámico. Por lo tanto, se decidió utilizar un enfoque experimental y análisis numérico para estudiar el comportamiento a fatiga de los morteros adhesivos industrializados tipo ACII y ACIII que componen el sistema de revestimiento cerámico, sometiéndolos a cargas cíclicas de tracción y compresión. En el enfoque experimental se realizaron ensayos de fatiga a tracción y compresión axial para los morteros ACII y ACIII, en los cuales los niveles de tensión para la realización de los ensayos de fatiga fueron definidos a partir de los resultados obtenidos en los ensayos de caracterización de resistencia a tracción en flexión y compresión axial de estos morteros. Los resultados de los ensayos de fatiga permitieron la elaboración de la curva S-N o curva de Wöhler, lo que permitió obtener el límite de ruptura por resistencia a la fatiga de los morteros ACII y ACIII.

Palabras clave: Desprendimiento del Revestimiento Cerámico. Fatiga. Mortero.

1 INTRODUCTION

Problems with the ceramic coating system can range from simple blooms to complete displacement of the ceramic pieces. In this sense, Bowman and Westgate [1] emphasize that the emergence of pathological manifestations is not related to a single cause, but to a sum of factors. It is also observed that the quality and durability of ceramic tiles are strongly linked to planning, choice of materials, construction quality and maintenance throughout their useful life.

Fiorito [2] emphasizes that, in fact, the expression coating structure should be used. In this system, the coating support layers have their own deformations, in addition, in the case of ceramic coating, they can deform depending on humidity and thermal variation in the environment, among other factors. It may also happen that, with the progressive increase in efforts, a state of tension is reached and the covering parts may fracture. In another case, due to the presence of compression stresses, a buckling process will occur, leaving the coating irreparably detached and even causing the coating to peel off (Fig. 1).

Figure 1

Ceramic coating peeling off on facades [7]

Fiorito [2] mentions that the peeling of the ceramic coating is quite common. This pathological manifestation can be caused by numerous factors, such as:

- low adhesion between system layers;
- expansion, due to humidity, of ceramic pieces;
- excessive shrinkage of the mortar, causing cracks that will lead to a future loss of adhesion of the coating layers; and
- emergence of stresses resulting from thermal effects that can rupture the ceramic coating system due to fatigue.

Therefore, the objective of this research is to analyze the behavior of stresses in samples subjected to cyclic loads, with the aim of tracing the S-N Curve of fatigue traction and compression of industrialized adhesive mortars of the ACII and ACIII types.

2 EXPERIMENTAL MATERIALS AND PROCEDURES

2.1 PREPARATION OF ACII AND ACIII ADHESIVE MORTARS

Industrialized adhesive mortars of the ACII and ACIII types were used, obtained on the local market, sold in 20 kg packages. It is worth noting that these mortars are widely used for laying ceramic tiles on facades in the Federal District.

The preparation of industrialized adhesive mortars was carried out in accordance with ABNT NBR 14081 [3]. In the mixing process, for the ACII adhesive mortar, the water/mortar ratio was maintained at 0.22, and for the ACIII adhesive mortar, the water/mortar ratio was equal to 0.28, within the ranges recommended by the manufacturer.

Homogenization was carried out in a quantity of 20 kg of dry mortar, using a low-speed mixer until a workable consistency was obtained, as shown in Fig. 2. The mixing time was 2 minutes and a time interval of 15 minutes for maturation, which represents the time needed for the additives to begin their action, and then another 1 minute for the final mixture, according to the specification recommended by the manufacturer of adhesive mortars.

Figure 2

Mixer and stages of the adhesive mortar preparation process

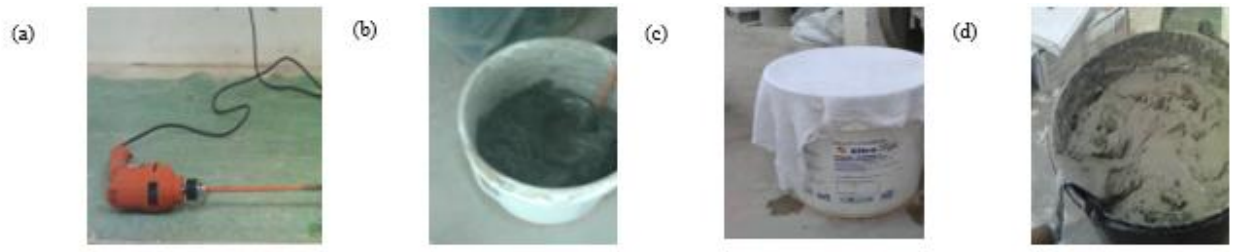

2.2 CHARACTERIZATION OF ADHESIVE MORTARS

The mechanical properties were determined using the procedures of the ABNT NBR 13279:2005 standard [4], which specifies the testing methods for tensile strength in flexion and axial compression, as there is no specific standard for this purpose for adhesive mortars.

2.2.1 Flexural tensile strength test

The flexural tensile strength test consists of applying a load centered on the bi-supported prismatic specimen until it ruptures through flexion. For this test, a manual press was used, as illustrated in Fig. 3.

Figure 3

Flexural tensile strength test

Flexural tensile strength is determined using Equation 1.

$$R_f = \frac{1{,}5F_fL}{40^3} \quad (1)$$

Where:

- R_f is the flexural tensile strength, in MPa;
- F_f is the load applied vertically at the center of the prism, in N; and
- L is the width between the supports, in mm.

Table 1 illustrates the results of the characterization tests of the industrialized adhesive mortars ACII and ACIII in the hardened state on their flexural tensile strength, the results of which obtained correspond to the average absolute deviation of the specimens tested after 28 days, according to the NBR 13279:2005 standard.

Table 1

Result of the rupture stress of the tensile test in bending ACII and ACII

Property	Results	
Adhesive mortars	ACII	ACIII
Flexural tensile strength (MPa)	3,77	3,26

2.2.2 Axial compression resistance test

Initially, halves of the three specimens from the flexural tensile strength test were used, positioning them in the support device in the manual press, as shown in Fig. 4, so that the flat face would not be in contact with the support device or the press loading device. Then, a load was applied at a speed of (500 ± 50) N/s until the specimen ruptured.

Figure 4

Axial compression resistance test

Axial compressive strength is calculated using Equation 2.

$$R_c = \frac{F_c}{1600} \quad (2)$$

Where:

- R_c is the compressive strength, in MPa;
- F_c is the maximum applied load, in N; and
- 1600 is the section area, considered square of the 40 mm x 40 mm load device, in mm².

In Table 2, the compressive strength results of industrialized adhesive mortars ACII and ACIII are presented, at 28 days of age, in accordance with the NBR 13279 standard [4].

Table 2

Result of the rupture stress of the compression test of ACII and ACIII

Property	Results	
Adhesive mortars	ACII	ACIII
Compressive strength (MPa)	10,91	9,68

2.3 DYNAMIC TESTING OF ADHESIVE MORTARS

Dynamic tests represent fatigue tests and can be in tension, compression, or in stress states varying between tension and compression. Considering that, as yet, there are no standards drawn up for carrying out specific fatigue testing of adhesive mortars, this methodology was based on fatigue tests carried out by Cervo [5] for concrete.

The fatigue test consists of applying a cyclic load to an appropriate test specimen sized according to the type of test to be carried out. The fatigue test is capable of providing quantitative data regarding the characteristics of a material or component when supporting, for a long period and without breaking, cyclic loads. The main results of the fatigue test are: the fatigue resistance limit (σ_{Rf}), which corresponds to a stress limit, such that, for values below this limit, the specimen will never suffer fatigue failure; the fatigue resistance (σ_f), which corresponds to the stress at which the specimen ruptures for an arbitrary number of load application cycles; and fatigue life (N_f) consists of the number of cycles that will cause failure for a given stress level [6].

In the experimental tensile and compressive strength test, the material's resistance limit is determined as a function of the maximum load reached during the characterization test, after which the material ruptures. It is therefore established that the material does not break with a load lower than that subjected to static stress. However, when dynamic, repeated or fluctuating stresses are applied to a given material, it may break with a load much lower than the maximum load reached during the static tensile or compression test. In this case, there is the so-called fatigue rupture of the material.

For the fatigue resistance tests, a universal testing machine was used, as illustrated in Fig. 5, in which the test can be operated with tension or displacement control that occurs through a hydraulic device.

Figure 5

Universal testing machine

This machine is controlled using a computer, and through this the pump and hydraulic actuator are activated to carry out the test. The clamping claws for the specimens are also hydraulically driven, so that the pressure on them can be varied, using a controller at the base of the machine itself. The machine also has a load cell that measures the force applied to the specimens in a range from 1 KN to 100 KN.

In the fatigue resistance tests, prismatic specimens were sized for the tensile test using the geometric stress concentration factor [7], as shown in Fig. 6 (a). For the compression test, cylindrical specimens were used, measuring 10 cm in diameter and 20 cm in height, as shown in Fig. 6 (b).

Figure 6

a) prismatic specimen assembled for the tensile fatigue test; (b) cylindrical specimen assembled for the compression fatigue test

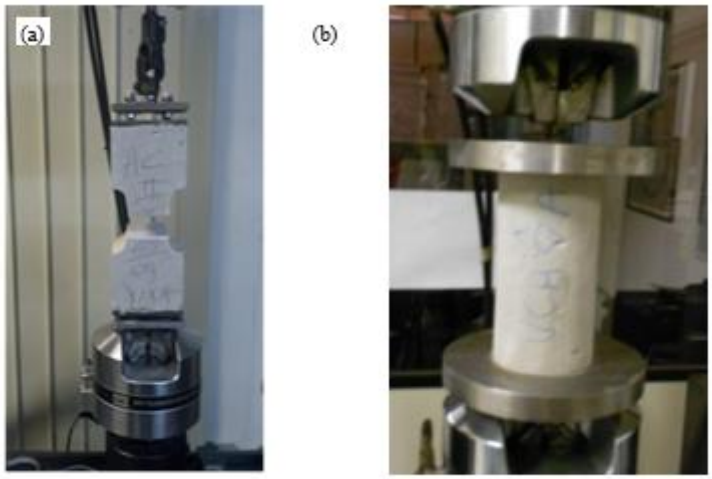

3 EXPERIMENTAL RESULTS

Based on the results of the flexural tensile strength test of mortars ACII (3.77 MPa) and ACIII (3.26 MPa), which correspond to the average absolute deviation of the specimens tested after 28 days, according to ABNT NBR 13279 [4], the loads for the axial tensile fatigue tests of ACII and ACIII were calculated, following as a reference the fatigue standard for steel ASTM E 468-11[8], as shown in Fig.7 and Fig. 8.

Figure 7

Load sizing for the axial tensile fatigue tests of the Colante ACII mortar

BASE = DxE		
D=Largura	12,00	[cm]
E=Espessura	12,00	[cm]
CORPO = dxE		
r/d =	0,275	adm
d = D-2r	7,74	[cm]
r =	2,13	[cm]
K_t - Ábaco	1,60	adm
A1 = BASE = Área Maior	144,00	[cm²]
A2 = CORPO = Área Menor	92,90	[cm²]
Tensão àTração-Máx-Arg. Col. ACII =	**3,77**	**MPa**
Tensão àTração-Máx-Arg. Col. ACII =	0,37	[kN/cm²]
Força à tração-Máx-Arg. Col. ACII =	34,37	[kN]
Faixa de trabalho da Máquina MTS 810		
Mín =	1,00	[kN]
Máx =	100,00	[kN]
Níveis do TESTE		
Valores Usado para o Ensaio da fadiga		
1,0*Ft	34,37	[kN]
0,9*(0,8)*Ft	24,75	[kN]
0,7*(0,8)*Ft	19,25	[kN]
0,3*(0,8)*Ft	8,25	[kN]

Figure 8

Dimensioning of loads for axial tensile fatigue tests of ACIII adhesive mortar

BASE = DxE		
D=Largura	12,00	[cm]
E=Espessura	12,00	[cm]
CORPO = dxE		
r/d =	0,275	adm
d = D-2r	7,74	[cm]
r =	2,13	[cm]
K_t - Ábaco	1,60	adm
A1 = BASE = Área Maior	144,00	[cm²]
A2 = CORPO = Área Menor	92,90	[cm²]
Tensão à Tração-Máx-Arg. Col. ACIII =	**3,26**	**MPa**
Tensão à Tração-Máx-Arg. Col. ACIII =	0,32	[kN/cm²]
Força à Tração-Máx-Arg. Col. ACIII =	29,73	[kN]
Faixa de trabalho da Máquina MTS 810		
Mín =	1,00	[kN]
Máx =	100,00	[kN]
Níveis do TESTE		
Valores Usado para o Ensaio da fadiga		
1,0*Ft	29,73	[kN]
0,9*(0,8)*Ft	21,40	[kN]
0,7*(0,8)*Ft	16,65	[kN]
0,3*(0,8)*Ft	7,13	[kN]

Table 3 and Table 4 illustrate the results of the axial tensile fatigue tests for the ACII and ACIII mortars, respectively, presenting the values of load, tension (S) at the adopted axial tension and the number of cycles (N) performed.

Table 3

Axial tensile fatigue test of ACII adhesive mortar

Force (kN)	Area (cm²)	Tension (MPa)	Number of cycles	Situation
6,00	92,90	0,71	4.213	Broke
6,00	92,90	0,71	4.473	Broke
5,50	92,90	0,61	1.213.388	Not broke
5,50	92,90	0,61	1.045.456	Not broke
5,00	92,90	0,51	1.031.194	Not broke
4,88	92,90	0,51	1.022.125	Not broke
4,88	92,90	0,51	1.027.123	Not broke

Seven axial tensile fatigue tests were carried out for the ACII mortar (Table 3). In five of the tests carried out, the specimen did not rupture until the number of cycles above 1 million, when the decision was made to stop the test and it was assumed that rupture would no longer occur. These tests were carried out with a load of 4.88 kN, 5.00 kN and 5.50 kN and tension of 0.51 MPa and 0.61 MPa, respectively. In the fifth test carried out, a load of 6.00 kN and tension of 0.71 MPa were chosen. This load value was defined based on the characterization test of the flexural tensile strength of the ACII mortar, presented in Fig. 7 and whose value was obtained as 3.77 MPa. In this case, the ACII mortar ruptured in the axial tensile fatigue test and rupture occurred after 4,473 cycles.

The S-N or Wöhler curve, showing the behavior of ACII when subjected to cyclic stresses to obtain axial tensile fatigue resistance (Fig. 9).

Figure 9

ACII tensile fatigue S-N curve

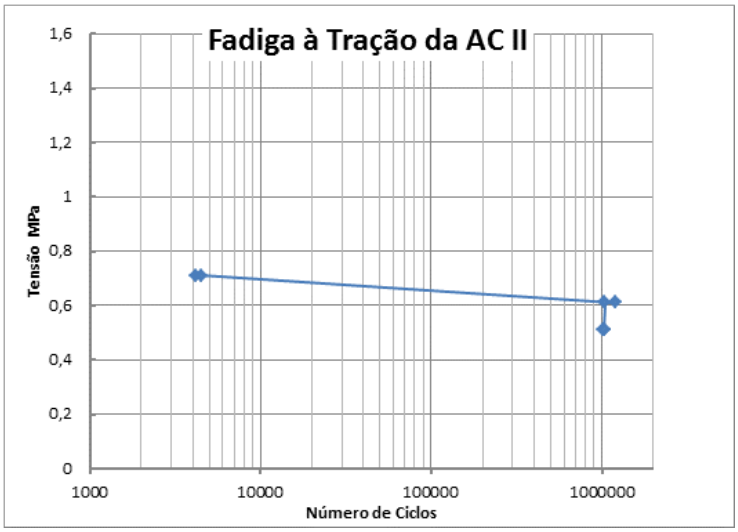

Six axial tensile fatigue tests were carried out for the ACIII mortar (Table 4). In three of the tests carried out, the test piece did not break until the number of cycles above 1 million,

when, in the same way as for the tests carried out with the industrialized adhesive mortar ACIII, it was decided to stop the test and assume that the rupture would no longer occur. These tests were carried out with a load of 8.50 kN and 9.00 kN and tension of 0.92MPa and 1.02MPa, respectively. In the fourth test carried out, a load of 10.00kN and tension of 1.12MPa were chosen. This load value was defined as 34.35% of the axial tensile failure load of the ACIII based on the characterization test of its flexural tensile strength, presented in Fig. 8 and whose value obtained was 3.26MPa. In this case, the ACIII mortar ruptured in the axial tensile fatigue test, occurring after 87,526 cycles.

Table 4

ACIII axial tensile fatigue test

Force (kN)	Area (cm²)	Tension (MPa)	Number of cycles	Situation
10,32	92,90	1,22	1.979	Broke
10,00	92,90	1,12	62.517	Broke
10,00	92,90	1,12	87.526	Broke
9,00	92,90	1,02	1.076.778	Not broke
9,00	92,90	1,02	1.062.537	Not broke
8,50	92,90	0,92	1.045.541	Not broke

The S-N or Wöhler curve showing the behavior of ACIII mortar when subjected to cyclic stresses to obtain axial tensile fatigue resistance (Fig. 10).

Figure 10

Tensile fatigue S-N curve of ACIII

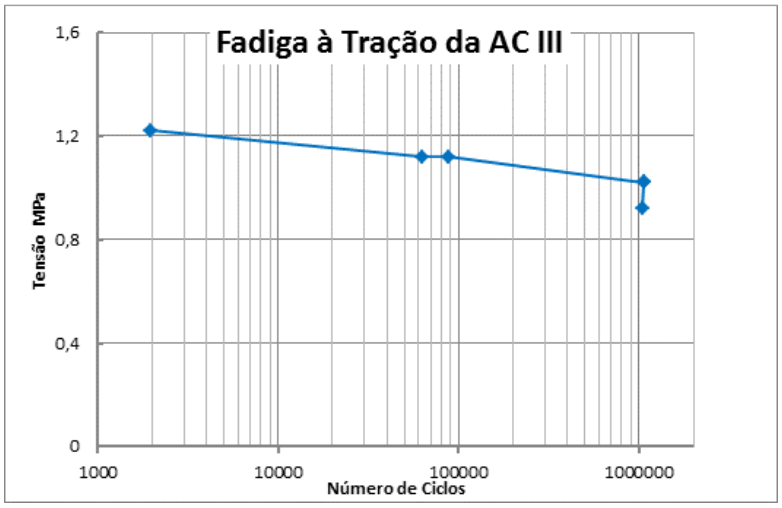

3.2 COMPRESSION FATIGUE TEST RESULTS

Given the results of the axial compression resistance tests of mortars ACII (10.91 MPa) and ACIII (9.68 MPa), which correspond to the average absolute deviation of the specimens tested after 28 days, in accordance with the ABNT standard NBR 13279 [4], the loads for the compression fatigue tests of these mortars were calculated, following as a reference the fatigue standard for steel ASTM E 468-11 (Fig. 11 and Fig. 12).

Figure 11

Dimensioning of loads for axial compression fatigue tests of ACII adhesive mortar

BASE = πr²		
r=	5,00	[cm]
π=	3,14	adm
CORPO = πr²		
Área do CP	78,54	[cm²]
Tensão à Compressão-Máx-Arg. Col. ACII =	**10,91**	**MPa**
Tensão à Compressão-Máx-Arg. Col. ACII =	1,07	[kN/cm²]
Força à Compressão-Máx-Arg. Col. ACII =	84,04	[kN]
Faixa de trabalho da Máquina da MTS 810		
Mín =	1,00	[kN]
Máx =	100,00	[kN]
Níveis do TESTE		
Valores Usado para o Ensaio da fadiga		
1,0*Ft	84,04	[kN]
0,9*(0,8)*Ft	60,51	[kN]
0,7*(0,8)*Ft	47,06	[kN]
0,3*(0,8)*Ft	20,17	[kN]

Figure 12

Dimensioning of loads for axial compression fatigue tests of ACIII adhesive mortar

BASE = πr²		
r=	5,00	[cm]
π=	3,14	adm
CORPO = πr²		
Área do CP	78,54	[cm²]
Tensão à Compressão-Máx-Arg. Col. ACIII =	**9,68**	**MPa**
Tensão à Compressão-Máx-Arg. Col. ACIII =	0,95	[kN/cm²]
Força àCompressão-Máx-Arg. Col. ACIII =	74,61	[kN]
Faixa de trabalho da Máquina MTS 810		
Mín =	1,00	[kN]
Máx =	100,00	[kN]
Níveis do TESTE		
Valores Usado para o Ensaio da fadiga		
1,0*Ft	74,61	[kN]
0,9*(0,8)*Ft	53,72	[kN]
0,7*(0,8)*Ft	41,78	[kN]
0,3*(0,8)*Ft	17,91	[kN]

Table 5 and Table 6 illustrates the results of the axial compression fatigue tests for the ACII and ACIII mortars, respectively, presenting the values of load, tension (S) at the adopted axial compression and the number of cycles (N) performed.

Seven axial compression fatigue samples were tested for the ACII mortar (Table 5). In three samples, the tests were carried out with a load of 39.00 kN and tension of 5.00 MPa, the test piece did not break until the number of cycles above 1 million, when the decision was made to stop the test and assume it was assumed that the rupture would no longer occur. Then, four tests were carried out with loads of 45.00KN, 66.00kN and 80.00KN with stresses of 5.10MPa, 8.56MPa and 10.38MPa respectively. This load value was defined based on the characterization test of the axial compression resistance of the ACII mortar, presented in Fig. 11 and whose value obtained was 10.91 MPa. In these cases, the ACII ruptured in the axial compression fatigue test and the rupture occurred, respectively, with 345,890, 283,439 and 271,581 cycles. Furthermore, another test was carried out with a load of 80.00 kN and a tension of 10.38MPa. In this case, there was also rupture and it occurred with 236,848 cycles, which is a smaller number of cycles than that obtained for tests with load of 66.00 kN and tension of 8.56MPa.

Table 5

Result of the ACII compression fatigue test

Force (kN)	Area (cm²)	Tension (MPa)	Number of cycles	Situation
80,00	78,54	10,38	236.848	Broke
66,00	78,54	8,56	271.581	Broke
66,00	78,54	8,56	283.439	Broke
45.00	78,54	5,10	345.890	Broke
39,00	78,54	5,00	1.051.637	Not Broke
39,00	78,54	5,00	1.086.048	Not Broke
39,00	78,54	5,00	1.092.080	Not Broke

Fig. 13 illustrates the S-N or Wöhler curve showing the behavior of ACII mortar when subjected to cyclic stresses to obtain fatigue resistance to axial compression.

Figure 13

Compression fatigue S-N curve of ACII mortar

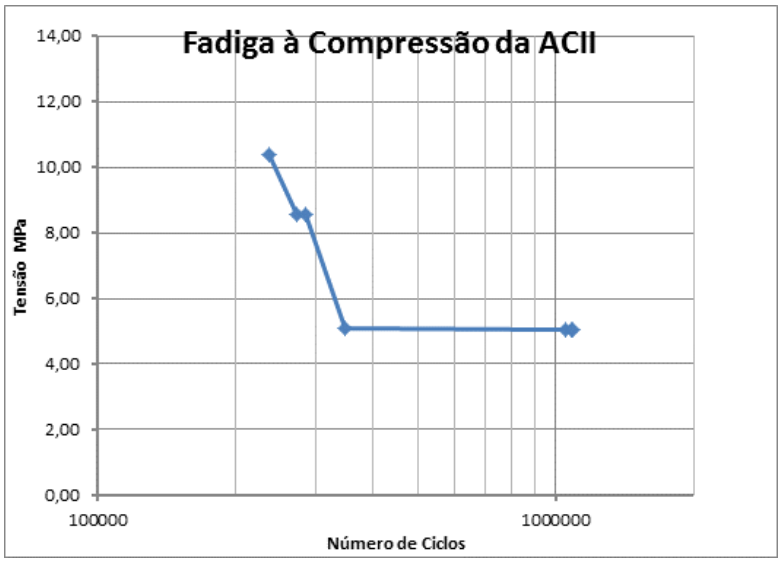

Seven axial compression fatigue tests were carried out for the ACIII mortar (Table 6). In three of the tests carried out with loads of 55.00KN and 60.00kN with tensions of 7.13MPa and 7.75MPa respectively, the test piece did not break until the number of cycles above 1 million, when the decision was made to stop the test and it was assumed that the rupture would no longer occur. Then, a test was carried out with a load of 65.00 kN and tension of 8.46MPa where the ACIII mortar ruptured and this occurred after 328,604 cycles. This load value of 65.00 kN was defined based on the ACIII axial compression resistance characterization test, presented in Fig. 14 and whose value obtained was 9.68 MPa. Finally, two tests were carried out with a load of 70.00 kN and a tension of 9.07MPa. In these cases, the ACIII ruptured in the axial compression fatigue test and the rupture occurred after 36,968 and 62,660 cycles.

Table 6

Result of the compression fatigue test of the ACIII mortar

Force (kN)	Area (cm²)	Tension (MPa)	Number of cycles	Situation
70,00	78,54	9,07	36.968	Broke
70,00	78,54	9,07	62.660	Broke
65,00	78,54	8,46	298.632	Broke
65,00	78,54	8,46	328.604	Broke
60,00	78,54	7,75	1.018.584	Not Broke
60,00	78,54	7,75	1.056.984	Not Broke
55,00	78,54	7,13	1.040.196	Not Broke

Fig. 14 shows the S-N or Wöhler curve showing the behavior of ACIII when subjected to cyclic stresses to obtain fatigue resistance to axial compression.

Figure 14

S-N curve of ACIII compression fatigue

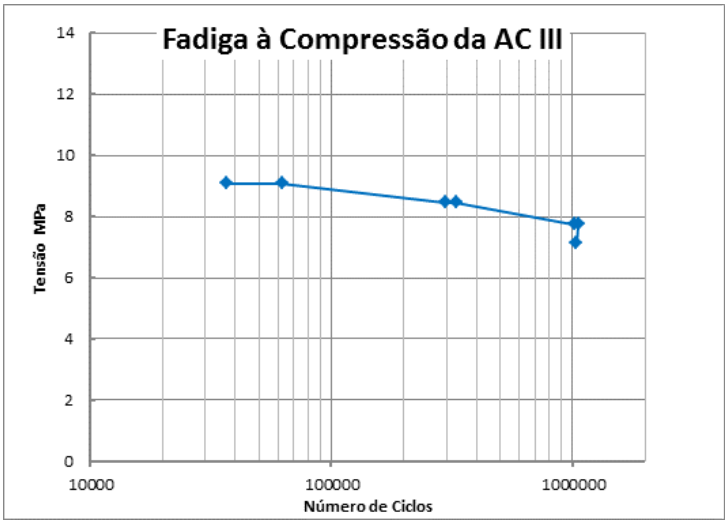

4 S-N OR WÖHLER CURVES FOR ACII AND ACIII

To determine the capacity of ACII and ACIII industrialized adhesive mortars to resist a set of repetitive compression and tension efforts, the methodology worked by Cervo [5] was adopted as a basis, which identified the compression and tension S-N fatigue curves for the concrete. Therefore, Equation 3 presented by Cervo [5] and Tepfers and Kutti [9] and the experimental test data presented in subitem 3 were used to determine the S-N (or Wöhler) curve of compression and tension fatigue for the industrialized adhesive mortars ACII and ACIII.

$$\frac{S}{f} = 1 - 0{,}0685(1 - R)logN \qquad (3)$$

4.1 COMPRESSIVE AND TENSILE FATIGUE S-N CURVES FOR ACII

Fig. 15 presents the S-N curves of compression and tension fatigue for the industrialized adhesive mortar ACII, generated from experimental test data (Table 3 and Table 5) and as already represented in Fig. 7 and Fig. 9.

Figure 15

ACII Compression and Tensile Fatigue S-N Curves

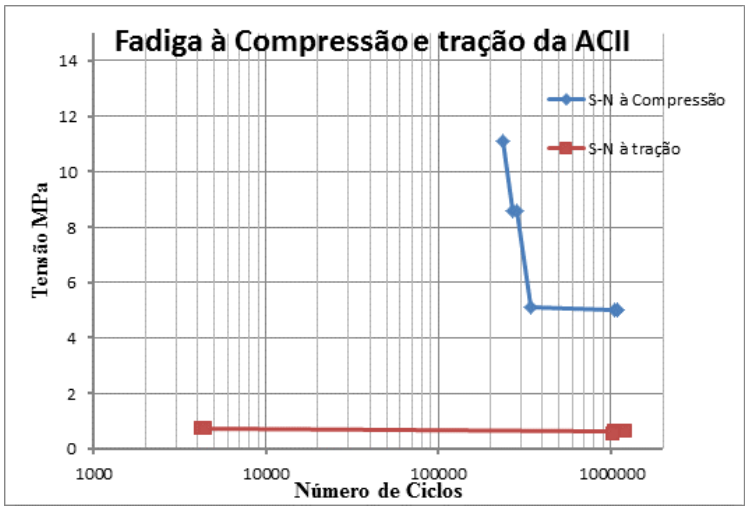

The S-N curves presented in Fig. 16 can also be linearized, where the “y” coordinate is the alternating stress in MPa; the abscissa “x” is the decimal logarithm of the number of cycles N (log(N)); and, S_{rc} and S_{rt} are, respectively, the fatigue resistance in a compression and tension test.

Figure 16

Linearized Compressive and Tensile Fatigue S-N Curves for ACII

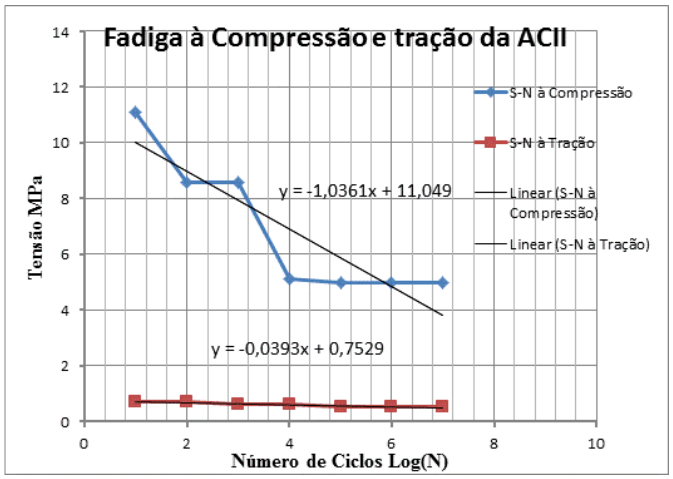

Considering the linearized curves in Fig. 16 and Equation 3 suggested by Cervo [5] and Tepfers and Kutti [9], it is possible to associate the variables “x” and “y” in the linearized equations in Fig. 16 as “log (N)” and “S”, respectively. For N > 106, the specimen does not break, as shown in the test results of subitem 3. In Equation 3, if R = 0 is considered and minimum stress is equal to 0 in the test, we have the following equations for ACII industrialized adhesive mortar.

Under compression:

For $N < 10^6 \rightarrow S = 11{,}049 - 1{,}0361 \log(N)$

For $N > 10^6 \rightarrow S = 4{,}83\ MPa$

Under traction:

For $N < 10^6 \rightarrow S = 0{,}7529 - 0{,}0393 \log(N)$

For $N > 10^6 \rightarrow S = 0{,}51\ MPa$

In a similar way to what was suggested by Cervo [5] and Tepfers and Kutti [9] for concrete, in Equation 3, a non-zero relationship R between the minimum and maximum stress, we have Equation 4 and Equation 5 for the compression and tensile fatigue test of the ACII industrialized adhesive mortar, respectively.

$$S = 11{,}049 - 1{,}0361(1 - R) \log(N) \quad (4)$$

$$S = 0{,}7529 - 0{,}0393(1 - R) \log(N) \quad (5)$$

To arrive at a more generic equation for the compression and tension fatigue of the ACII industrialized adhesive mortar, without depending on the values of the compression (f_{ck}) and tension (f_{tk}) stresses, Equations 4 and 5, respectively, must be divided. by values of f_{ck} and f_{tk} of the ACII adhesive mortar. These values are presented in Fig. 7 and Fig. 9, which are 10.91 MPa and 3.77 MPa. Thus, we have Equation 6 and Equation 7.

$$\frac{S}{f_{ck}} = 1{,}0127 - 0{,}0949(1 - R) \log(N) \quad (6)$$

$$\frac{S}{f_{tk}} = 0{,}1997 - 0{,}0104(1 - R) \log(N) \quad (7)$$

4.2 COMPRESSIVE AND TENSILE FATIGUE S-N CURVES FOR ACIII

Fig. 17 presents the S-N curves of compression and tension fatigue for the industrialized adhesive mortar ACIII, generated from experimental test data (Table 4 and Table 6) and as already represented in Fig. 8 and Fig. 10.

Figure 17

ACIII Compression and Tensile Fatigue S-N Curves

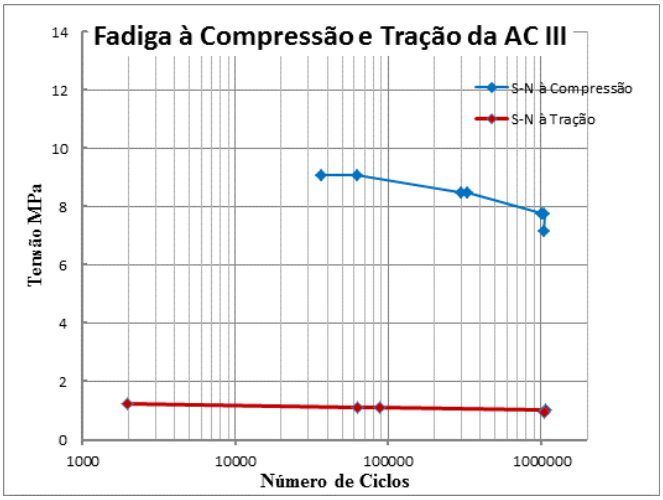

The S-N curves presented in Fig. 17 can also be linearized as shown in Fig. 18, where the “y” coordinate is the alternating stress in MPa; the abscissa “x” is the decimal logarithm of the number of cycles N (log(N)); and S_{rc} and S_{rt} are, respectively, the fatigue resistance in a compression and tension test.

Figure 18

Linearized Compressive and Tensile Fatigue S-N Curves for ACIII

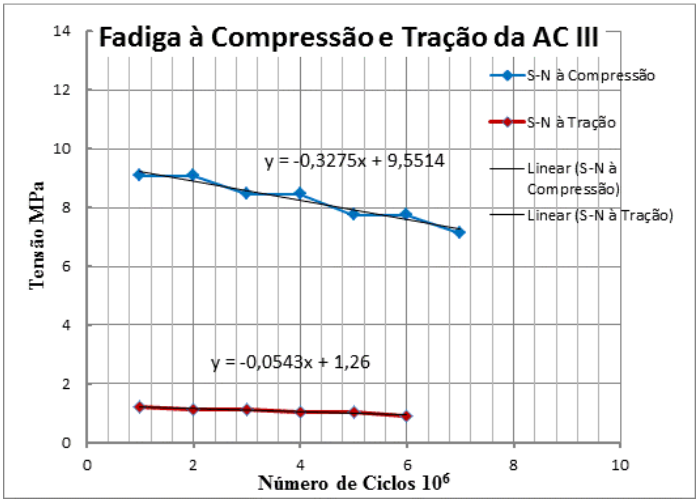

Considering the linearized curves in Fig. 18 and Equation 3 suggested by Cervo [5] and Tepfers and Kutti [9], it is possible to associate the variables “x” and “y” in the linearized equations in Fig. 18 as being “log (N)” and “S”, respectively. Knowing that for N > 106 the specimen does not broke, as shown in the test results of subitem 3 and, also, in Equation 3,

if R = 0 is considered, since in the test the minimum stress is “0”, we have the following equations for the industrialized adhesive mortar ACIII.

Under compression:

For $N < 10^6 \rightarrow S = 9{,}5514 - 0{,}3275 \log(N)$

For $N > 10^6 \rightarrow S = 7{,}58\ MPa$

Under traction:

For $N < 10^6 \rightarrow S = 1{,}2600 - 0{,}0543 \log(N)$

For $N > 10^6 \rightarrow S = 0{,}93\ MPa$

In a similar way to what was suggested by Cervo [5] and Tepfers and Kutti [9] for concrete (Equation 3) and considering a non-zero relationship R between the minimum and maximum stress, we have Equation 8 and Equation 9 for the compression and tensile fatigue test of industrialized ACIII adhesive mortar, respectively.

$$S = 9{,}5514 - 0{,}3275(1 - R) \log(N) \quad (8)$$

$$S = 1{,}2600 - 0{,}0543\ (1 - R) \log(N) \quad (9)$$

To arrive at a more generic equation for the compression and tension fatigue of the ACIII industrialized adhesive mortar and not depend on the values of the compression f_{ck} and tension f_{tk} stresses, Equation 8 and Equation 9 were divided, respectively, by f_{ck} and f_{tk} of ACIII presented in Table 4 and Table 6, that is, 9.68 MPa and 3.26 MPa. Thus, we have Equation 10 and Equation 11.

$$\frac{S}{f_{ck}} = 0{,}9867 - 0{,}0338(1 - R) \log(N) \quad (10)$$

$$\frac{S}{f_{tk}} = 0{,}3865 - 0{,}0166(1 - R) \log(N) \quad (11)$$

5 CONCLUSIONS

In this research, it was found that the fatigue resistance or fatigue limit (σf) in the axial tension of the ACII type adhesive mortar was 0.61 MPa. This value corresponds to 16.18% of the ACII flexural tensile strength value of the flexural tensile strength of 3.77 MPa.

The fatigue resistance or fatigue limit (σf) in axial tension of the ACIII adhesive mortar tested was 1.02 MPa. This corresponds to 31.00% of the ACIII flexural tensile strength value of the flexural tensile strength of 3.29 MPa.

The fatigue strength or fatigue limit (σf) in axial compression of ACII was 5.00MPa. This corresponds to 45.83% of the value of the axial compressive strength of the ACII adhesive mortar of the compressive rupture strength of 10.91 MPa.

The fatigue strength or fatigue limit (σf) in axial compression of ACIII was 7.75MPa. This means 80.06% of the value of the axial compressive strength of the ACIII adhesive mortar of the compressive rupture strength of 9.68 MPa.

REFERENCES

Bowman, R., & Westgate, P. (1992). Natural moisture behaviour of typical Australian ceramic tiles. In M. J. Bannister (Ed.), Ceramic, adding the value: Austceram 92. CSIRO Publications.

Fiorito, A. J. S. I. (1994). Manual de argamassa e revestimento: Estudo e procedimento de execução. Editora Pini.

Associação Brasileira de Normas Técnicas. (2012). NBR 14081: Argamassa colante industrializada para assentamento de placas cerâmicas. ABNT.

Associação Brasileira de Normas Técnicas. (2013). NBR 13529: Revestimento de paredes e tetos de argamassas inorgânicas — Terminologia. ABNT.

Cervo, T. C. (2004). Estudo da resistência à fadiga de concreto de cimento portland para pavimentação (Tese de doutorado). Escola Politécnica da Universidade de São Paulo.

Garcia, A., Spim, J. A., & Dos Santos, C. A. (2000). Ensaio dos materiais. LTC.

Uchôa, J. C. B., Bezerra, L. M., Bauer, E., Das Chagas, S. V. M., & Araújo, J. (2008). Análise experimental da resistência à fadiga de sistema de revestimento. In Anais do 50º Congresso Brasileiro do Concreto. IBRACON.

ASTM International. (2011). ASTM E468-11: Standard practice for presentation of constant amplitude fatigue test results for metallic materials. ASTM.

Tepfers, R., & Kutti, T. (1979). Fatigue strength of plain, ordinary and lightweight concrete. ACI Journal, 76(29), 635–652.